

Facile Hydrothermal Synthesis of CoFe₂O₄/Co₃O₄ Nanostructures for Efficient Oxygen Evolution Reaction

Pratik V. Shinde¹, Rutuparna Samal¹, Manoj Kumar Singh^{2,*},
Chandra Sekhar Rout^{1,*}

¹Centre for Nano and Material Sciences, Jain University, Jain Global Campus, Jakkasandra, Ramanagaram, Bangalore-562112, Karnataka, India

²Department of Physics under School of Engineering and Technology (SOET), Central University of Haryana (CUH), Mahendergarh- 123031, Haryana, India

*Corresponding authors, e-mail addresses: r.chandrasekhar@jainuniversity.ac.in; manojksingh@cuh.ac.in

Received 1 March 2021; accepted 25 March 2021; published online 30 March 2021

ABSTRACT

Co/Fe-based spinel oxide materials play an important role in the development of non-precious-metal-based electrocatalysts toward water splitting. Herein, we have synthesized the CoFe₂O₄/Co₃O₄ nanostructures via the facile hydrothermal method. CoFe₂O₄/Co₃O₄ nanostructures exhibited a low overpotential of 311 mV @10 mA/cm², a small Tafel slope of 87 mV/dec, as well as remarkable long-term stability towards OER. The performance of CoFe₂O₄/Co₃O₄ nanostructures is considerably higher than that of bare CoFe₂O₄ and Co₃O₄ materials. The outstanding performance is mainly attributed to the synergistic effect and increased active sites for OER reactions. This study can pave a pathway for engineering non-noble metal-based efficient, cost-effective, and durable electrocatalysts for OER.

1. INTRODUCTION

With the rapid depletion of fossil fuels and the associated environmental issues, the development of alternative clean energy sources is crucial. Numerous innovative, as well as trending concepts regarding energy storage/conversion, have recently been incorporated for achieving sustainable and environmental friendly systems such as water electrolysis, supercapacitors, fuel cells, and metal-air batteries. Electrochemical water splitting is considered as a promising approach among the above to obtain clean hydrogen fuels from renewable energy sources. The electrochemical splitting of water involves two crucial reactions, the cathode part involves hydrogen evolution reaction (HER) and the anode part ensues oxygen evolution reaction (OER) [1]. pH-dependent OER reaction is important owing to its impact on water splitting electrochemistry

wherein molecular oxygen is produced at the anode via several proton/electron transition reactions [2]. As OER involves a four-electron transfer process with the breaking of O-H bonds and the formation of O-O bonds, the reaction needs a high overpotential [3]. In-depth investigation for a suitable oxygen evolution electrocatalyst, substantial efforts have been devoted in recent times but meeting the practical application is still underway. Currently, Ru and Ir-based materials are the most efficient electrocatalysts for OER however, their cost and scarcity limit their large-scale practical applications [4, 5]. Both of the typical OER catalysts RuO₂ and IrO₂ oxidize to RuO₄ and IrO₃ respectively at the application of high anodic potential in acidic and alkaline electrolytes. Improvement in the electrocatalysts in terms of flexibility, production of high purity gases, low cost, high efficiency, and durability is highly

essential. Hence, extensive research efforts have been dedicated to the development of efficient electrocatalysts for the OER reactions. Earth-abundant materials have been widely used as electrocatalysts which demonstrated significant OER performance [6-8].

Considering chemical stability requirements towards the practical application, transition metal oxides can be looked upon as promising candidates. As compared to the single metal oxide, bimetal spinel oxides such as CoFe_2O_4 , NiFe_2O_4 , MnFe_2O_4 , etc., show significant electrocatalytic performance for oxygen evolution reaction [9-11]. Generally, spinel oxide structure is represented as AB_2O_4 , here A and B are metals in tetrahedral and octahedral sites, respectively [12]. The properties such as high abundance, low toxicity, rich redox chemistry, and superior stability make these class materials promising for energy applications [13, 14]. Precisely, cobalt ferrite (CoFe_2O_4) has gained particular interest in catalysis because of its earth abundance, environmental friendliness, high electrical conductivity, and sound durability [15, 16].

Herein, a simple hydrothermal method was adopted to prepare $\text{CoFe}_2\text{O}_4/\text{Co}_3\text{O}_4$ nanostructure. $\text{CoFe}_2\text{O}_4/\text{Co}_3\text{O}_4$ nanostructure exhibits a low overpotential of 311 mV at 10 mA/cm² for OER reaction. The as-prepared catalyst exhibited appreciable activity, a lower Tafel slope, and good stability in OER electrocatalysis. The present study offers a facile and efficient route to synthesize spinel metal oxides as a catalyst for high-performance OER reactions.

2. EXPERIMENTAL

2.1. Chemicals

The purities of all the reagents used are of analytical grade and used without further purification. Cobalt Nitrate [$\text{Co}(\text{NO}_3)_2 \cdot 6\text{H}_2\text{O}$] was purchased from Sisco Research Laboratories Pvt. Ltd., iron nitrate [$\text{Fe}(\text{NO}_3)_3 \cdot 9\text{H}_2\text{O}$], and urea [NH_2CONH_2] were procured from SD-Fine Chem Limited.

2.2. Synthesis

In a typical procedure for the preparation of $\text{CoFe}_2\text{O}_4/\text{Co}_3\text{O}_4$ material, cobalt nitrate (1.2 g), iron

nitrate (1.2 g), and urea (0.7 g) were dissolved independently in 20 mL distilled (DI) water. After 30 min stirring, solutions were mixed together and stirred for another 1 h at room temperature. Subsequently, the homogenous mixture was transferred into a 100 mL Teflon-lined stainless-steel autoclave and maintained at 120 °C for 16 h. After complete processing in a hot-air oven, the autoclave was cooled down to room temperature naturally. The obtained precipitate was washed several times with DI water and ethanol to remove any possible impurities and further dried in a vacuum oven at 90 °C for 6 h. Finally, as prepared $\text{CoFe}_2\text{O}_4/\text{Co}_3\text{O}_4$ material was calcined at 750 °C for 2 h in a muffle furnace. Additionally, CoFe_2O_4 and Co_3O_4 materials were also synthesized by following a similar procedure wherein, 0.8 g cobalt nitrate was used to prepare CoFe_2O_4 material while for Co_3O_4 preparation, iron nitrate source was eliminated.

2.3. Characterizations

The crystal structure of the synthesized powder was identified by a Rigaku Ultima IV X-ray diffractometer having Ni-filter for Cu K α radiation (wavelength, $\lambda = 1.541 \text{ \AA}$) at a scanning rate of 2°/min. Field emission scanning electron microscopy (FESEM) was performed with JEOL JSM-7100F, JEOL Ltd., Singapore to observe morphologies of the prepared materials. The energy dispersive spectrometer (EDAX) is equipped with a FESEM instrument used for the elemental analysis of the material. For understanding the functionalization of materials Fourier-transform infrared spectroscopy (FTIR) was recorded on the Perkin Elmer spectrophotometer using KBr pellets. The electrochemical study was performed on the CorrTest-CS350, China workstation.

2.4. Characterizations

Electrochemical measurements were performed within a three-electrode electrochemical cell with 0.5 M KOH electrolyte. Prepared electrocatalyst (2 mg) and Nafion solution (10 μL) were dispersed in isopropanol (200 μL) with the assistance of vigorous sonication (30 min) to form a homogeneous ink. The ink was then loaded onto a nickel foam in the area of 0.5 x 0.5 cm². The

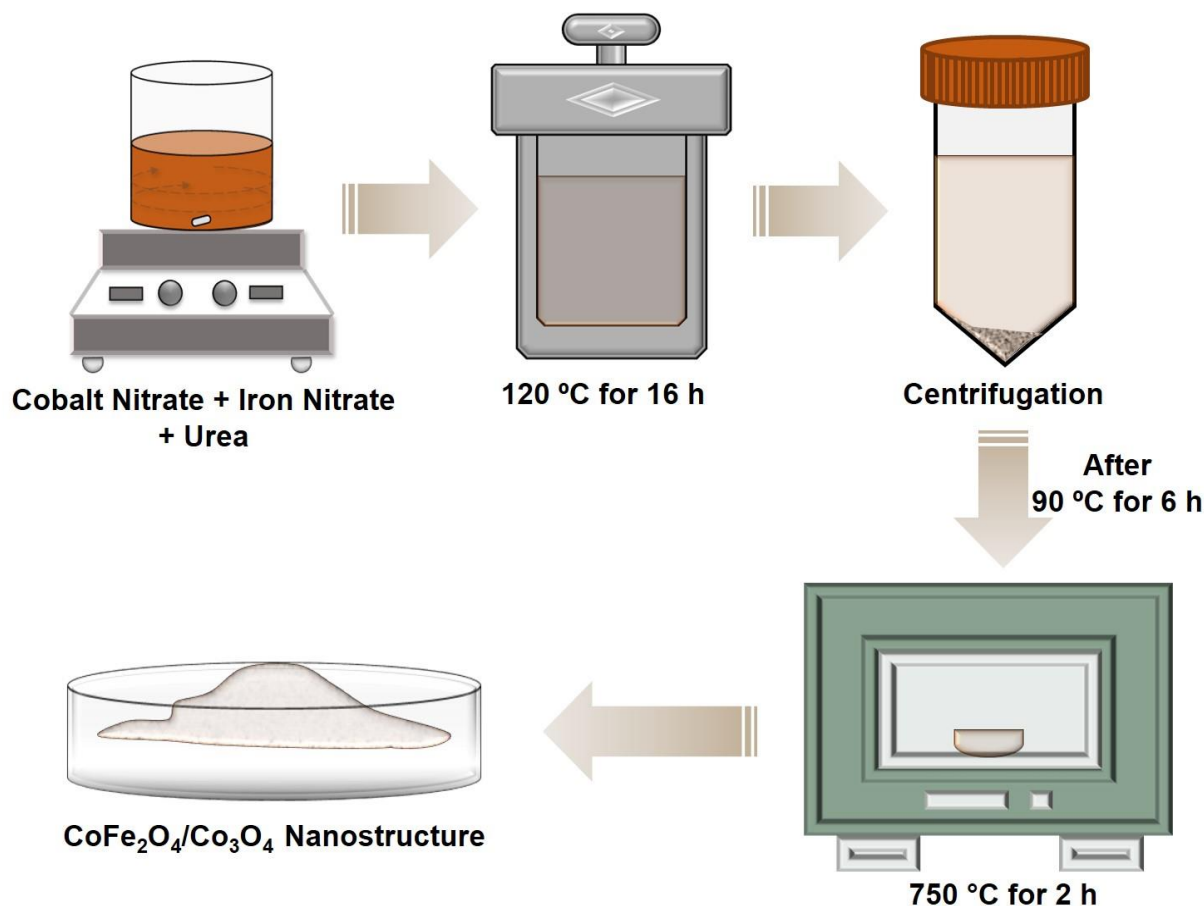


Figure 1. Schematic illustration of the synthesis of CoFe₂O₄/Co₃O₄ nanostructure.

Ag/AgCl electrode worked as the reference electrode, and a platinum wire was employed as an auxiliary electrode.

All the potentials reported in the present work have been converted to the reversible hydrogen electrode (RHE) using the following equation [3],

$$E_{(\text{RHE})} = E_{(\text{Ag}/\text{AgCl})} + 0.059 \text{ pH} + 0.197 \text{ V} \quad (1)$$

To evaluate the OER activity of as-prepared samples, linear sweep voltammetry (LSV) curves were recorded at a scan rate of 5 mV/s.

Tafel plots of overpotential vs. $\log(j)$ are fitted to the Tafel equation [3],

$$\eta = b \log |j| + a \quad (2)$$

where η is overpotential, j is the current density, and b is the Tafel slope.

Electrochemical impedance spectroscopy (EIS) was measured at an overpotential of 311 mV vs.

RHE in frequency ranges from 1 MHz to 0.01 Hz. Chronoamperometry was measured under a constant potential of 1.54 V vs. RHE over 10000 s.

3. RESULTS AND DISCUSSION

The schematic representation for the synthesis of CoFe₂O₄/Co₃O₄ nanostructures is illustrated in **Figure 1**. The CoFe₂O₄/Co₃O₄ nanostructures were prepared by a facile hydrothermal synthesis method using metal nitrate precursors followed by calcination in air.

3.1. Characterization

XRD measurement was employed to analyze the crystallographic phases of the synthesized materials. The obtained XRD patterns of the prepared catalyst are shown in **Figure 2**. The planes (111), (220), (311), (222), (400), (422), (511), and (440) correspond to the CoFe₂O₄ spinel structure. Whereas, the plane (111), (220), (311),

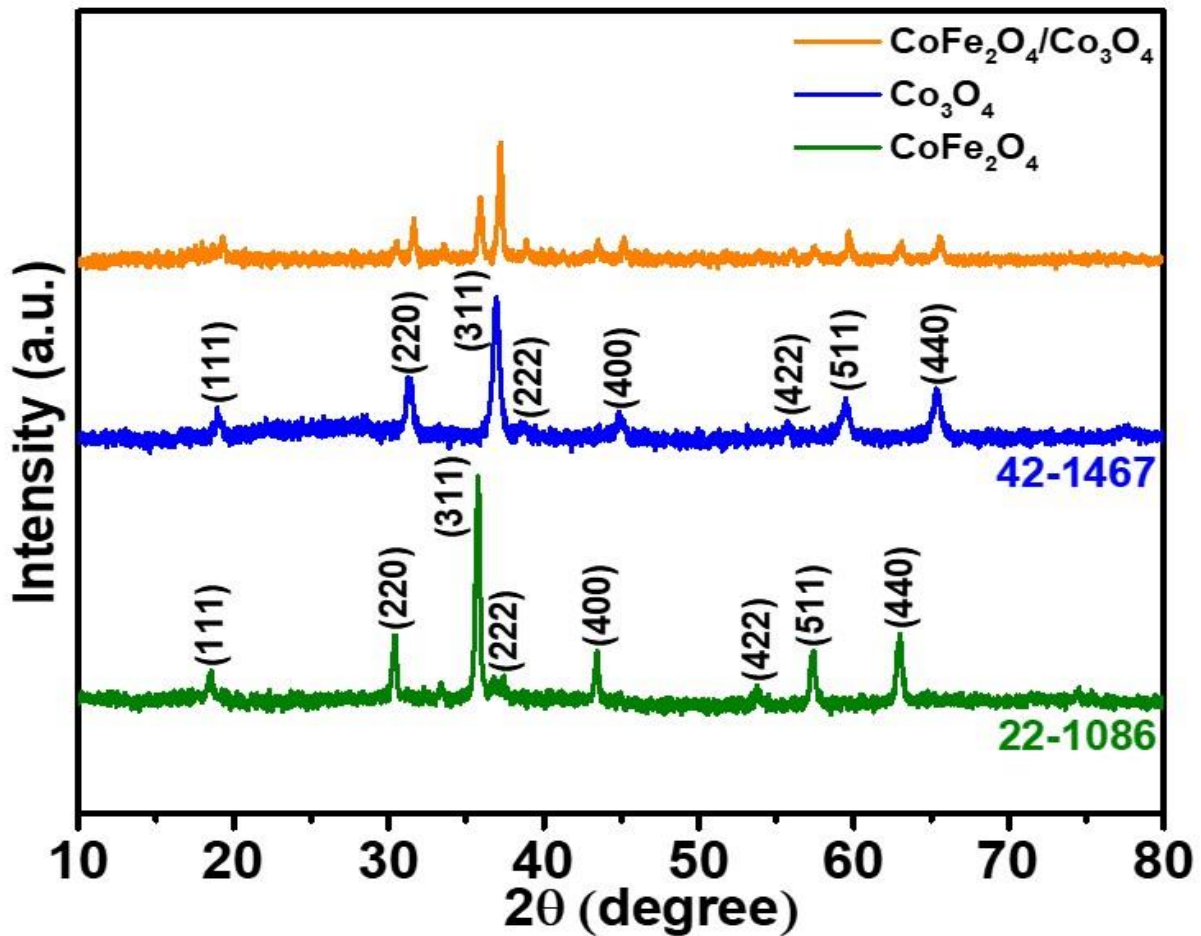


Figure 2. XRD patterns of the CoFe_2O_4 , Co_3O_4 and $\text{CoFe}_2\text{O}_4/\text{Co}_3\text{O}_4$ nanostructures.

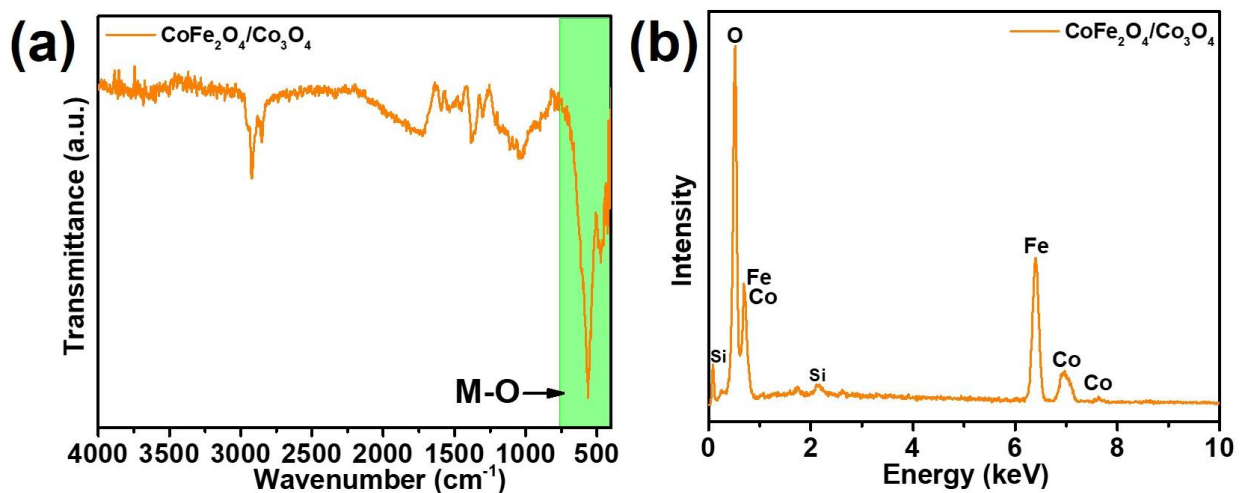


Figure 3. (a) FT-IR spectrum and (b) EDAX of the $\text{CoFe}_2\text{O}_4/\text{Co}_3\text{O}_4$ nanostructure.

(222), (400), (422), (511), and (440) can be ascribed to the Co_3O_4 . All of the diffraction peaks coincided with the standard values of cubic spinel CoFe_2O_4 (JCPDS no. 22-1086) and cubic Co_3O_4

(JCPDS no. 42-1467). Other than standard peaks, no secondary characteristic peaks of any type of impurities or other phases are detected. Clearly, we can perceive that $\text{CoFe}_2\text{O}_4/\text{Co}_3\text{O}_4$

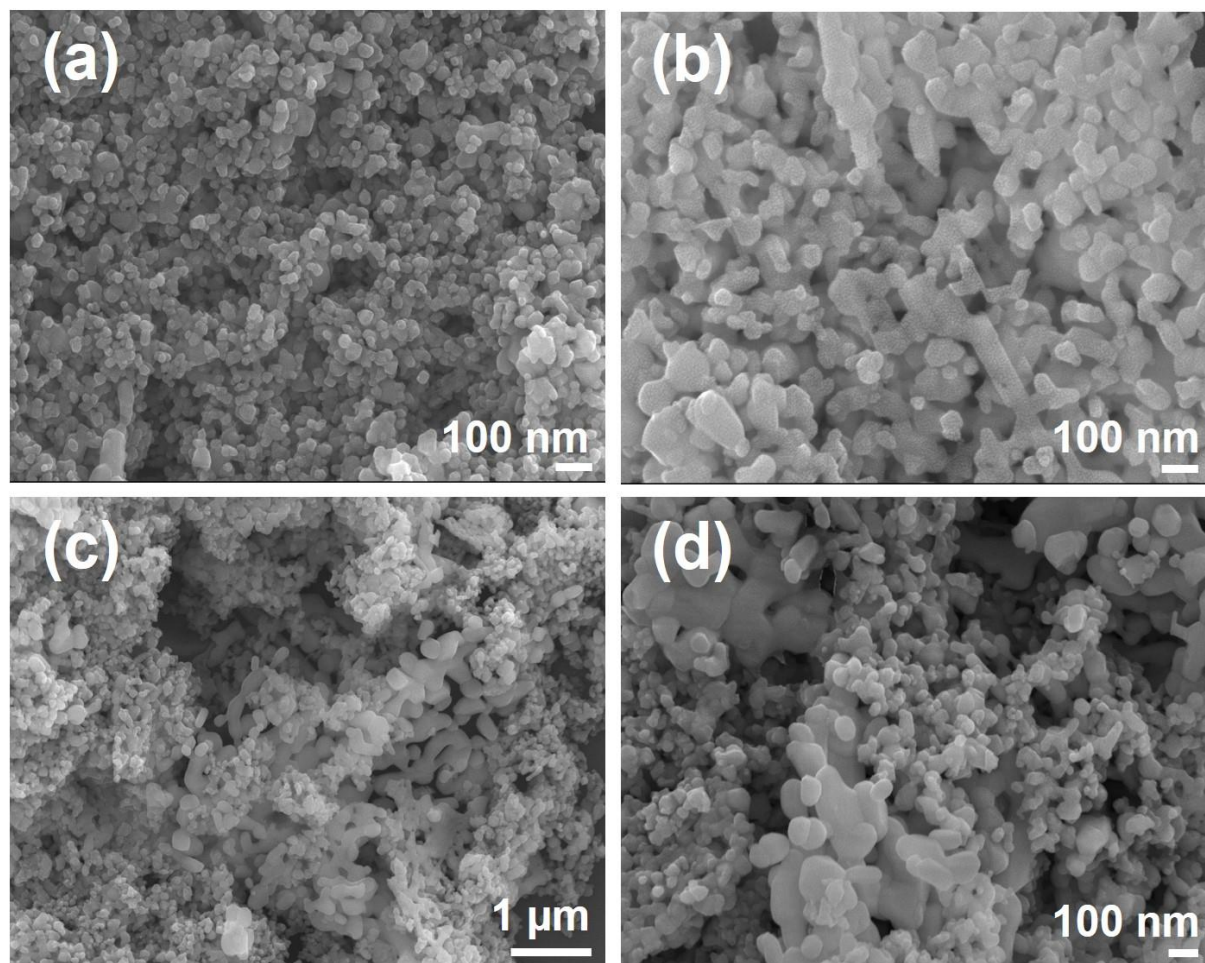


Figure 4. High resolution FE-SEM image of the (a) CoFe_2O_4 , (b) Co_3O_4 , (c-d) $\text{CoFe}_2\text{O}_4/\text{Co}_3\text{O}_4$ nanostructure.

nanostructures reveal the co-occurrence of CoFe_2O_4 and Co_3O_4 .

FT-IR spectroscopy is a useful tool to identify the functional group of the molecule. FT-IR spectrum of the $\text{CoFe}_2\text{O}_4/\text{Co}_3\text{O}_4$ nanostructure was recorded in the range of $450\text{--}4000\text{ cm}^{-1}$ (**Figure 3a**). The appearance of a peak in the range of $400\text{--}600\text{ cm}^{-1}$ is attributed to the metal-oxygen (M-O) stretching vibrations [17]. A sharp peak at around 1600 cm^{-1} and broadband near 3400 cm^{-1} is related to the deformation vibrations of adsorbed H_2O molecules and stretching vibrations of O-H on the catalyst surface, respectively [17-18]. Typical EDAX analysis of the resulted $\text{CoFe}_2\text{O}_4/\text{Co}_3\text{O}_4$ nanostructures is shown in **Figure 3b**, which indicated the existence of Co, Fe, and O elements. The morphologies and structural features of the synthesized CoFe_2O_4 , Co_3O_4 , and $\text{CoFe}_2\text{O}_4/\text{Co}_3\text{O}_4$ nanostructures were observed directly from the FE-

SEM images. **Figure 4a-d**, shows that the as-prepared $\text{CoFe}_2\text{O}_4/\text{Co}_3\text{O}_4$ sample inherits the multi-shape nanostructure morphology of the original CoFe_2O_4 and Co_3O_4 . EDAX mapping was performed to confirm the elemental composition of $\text{CoFe}_2\text{O}_4/\text{Co}_3\text{O}_4$ nanostructures. EDAX mapping reveals the uniform distribution of Co, Fe, and O as shown in **Figure 5a-d**. The atomic percentages of Co, Fe, and O elements were 27 %, 15 %, and 58 %, respectively.

3.2. Oxygen Evolution Reaction

The electrocatalytic behavior of as-prepared catalysts was then investigated by a three-electrode configuration in 0.5 M KOH electrolyte. LSV curves for oxygen evolution reaction are shown in **Figure 6a**. The required overpotential of $\text{CoFe}_2\text{O}_4/\text{Co}_3\text{O}_4$ nanostructure to achieve the

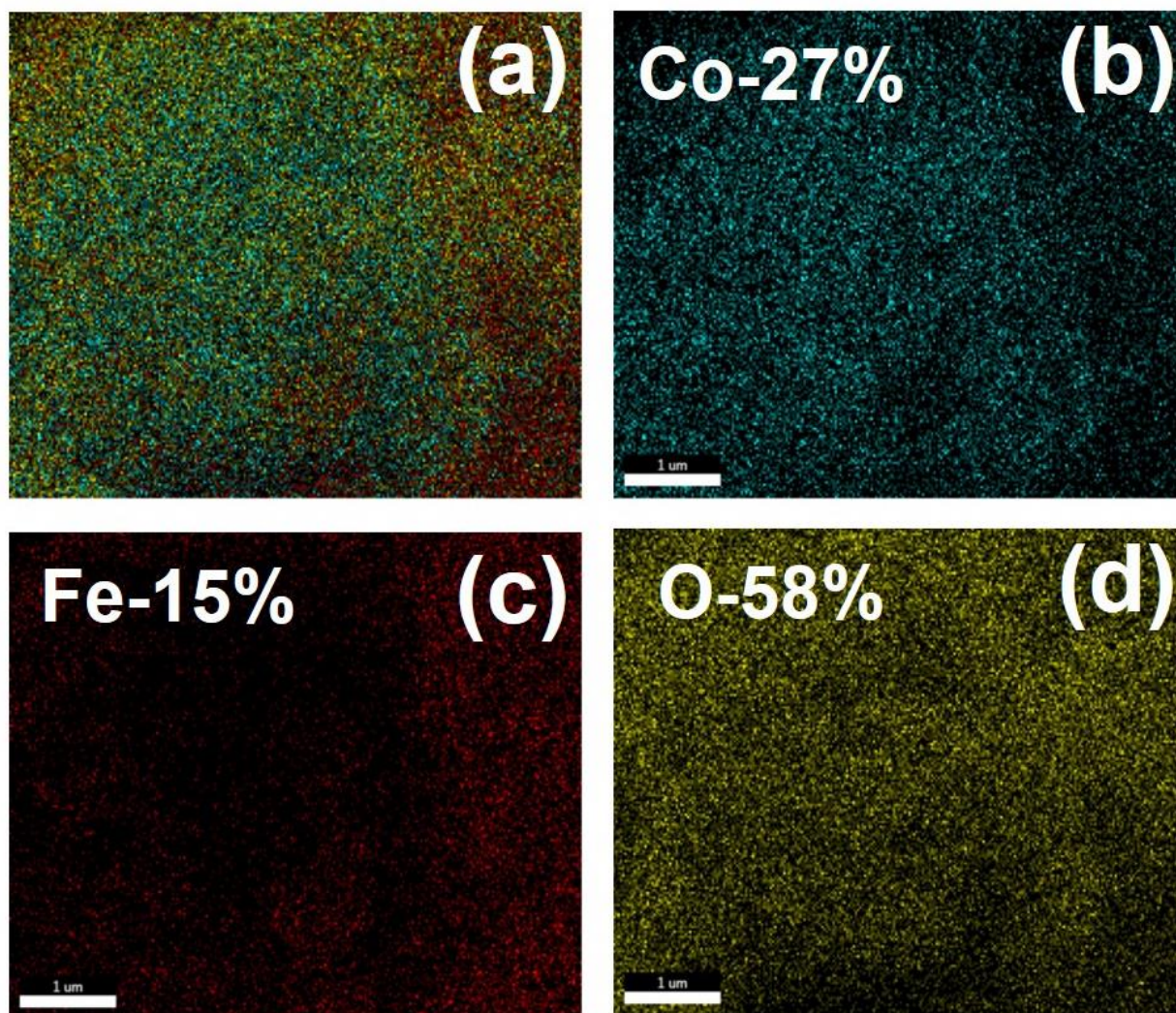


Figure 5. (a) Elemental mapping of the $\text{CoFe}_2\text{O}_4/\text{Co}_3\text{O}_4$, (b) Co, (c) Fe, (d) O.

active current density of 10 mA/cm^2 is only 311 mV, which is much lower than those of CoFe_2O_4 (351 mV), and Co_3O_4 (391 mV). The findings reveal that $\text{CoFe}_2\text{O}_4/\text{Co}_3\text{O}_4$ nanostructure demonstrated a remarkable activity towards OER reaction. A comparative Tafel plot was constructed by using the LSV graphs, to gain more insight into the kinetics of OER performance. For an electrocatalytically active catalyst, the smaller the value of the Tafel slope, the faster is the rate of reaction. **Figure 6b** illustrates the Tafel slope value of 141 mV/dec and 158 mV/dec derived for pure CoFe_2O_4 and Co_3O_4 , respectively. However, a relatively small Tafel slope value of 87 mV/dec is observed for $\text{CoFe}_2\text{O}_4/\text{Co}_3\text{O}_4$ nanostructure. Impressively, the estimated Tafel slope of $\text{CoFe}_2\text{O}_4/\text{Co}_3\text{O}_4$ nanostructure (87 mV/dec) is far better than those of the well-established OER catalysts such as RuO_2 (119 mV/dec). EIS was

used to examine the charge transfer kinetics of the working electrode. **Figure 6c** shows the Nyquist plots for pure CoFe_2O_4 , pure Co_3O_4 , and $\text{CoFe}_2\text{O}_4/\text{Co}_3\text{O}_4$ nanostructure, which were fitted to a simplified Randles circuit. A semicircle was observed in the high-frequency region and its diameter attributes to the charge transfer resistance (R_{ct}). A much lower solution resistance (R_s) and charge transfer resistance (R_{ct}) were observed over the $\text{CoFe}_2\text{O}_4/\text{Co}_3\text{O}_4$ nanostructure than that for pure CoFe_2O_4 and Co_3O_4 . A slow charge transfer resistance improved the electrical conductivity and hence EIS revealed that $\text{CoFe}_2\text{O}_4/\text{Co}_3\text{O}_4$ nanostructure exhibits high electrochemical performance for OER. Long-term stability is another key parameter to evaluate excellent OER electrocatalysts. To evaluate the durability of the $\text{CoFe}_2\text{O}_4/\text{Co}_3\text{O}_4$ nanostructure in the process of OER, chronoamperometry tests

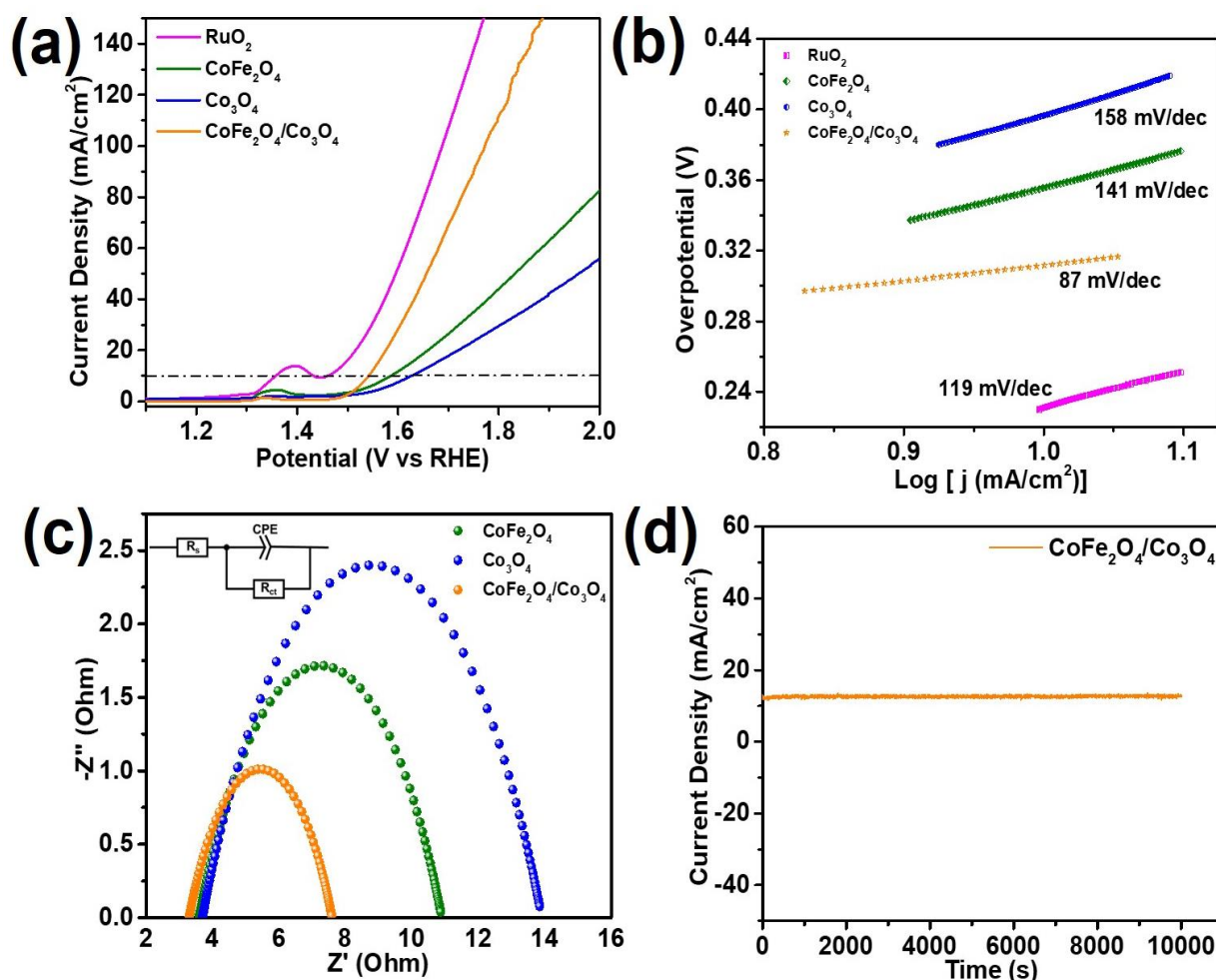


Figure 6. Electrocatalytic performance: (a) LSV curves, (b) Corresponding Tafel slopes, (c) Nyquist's plots, Inset: Randle's circuit, (d) Chronoamperometry plot at a potential of 1.54 V.

Table 1. OER performance of synthesized $\text{CoFe}_2\text{O}_4/\text{Co}_3\text{O}_4$ nanostructure catalyst and RuO_2 .

Sr. No.	Electrocatalyst	Overpotential (mV) @10 mA/cm ²	Tafel Slope (mV/dec)
1	RuO_2	236	119
2	CoFe_2O_4	351	141
3	Co_3O_4	391	158
4	$\text{CoFe}_2\text{O}_4/\text{Co}_3\text{O}_4$	311	87

were performed at 1.54 V vs. RHE as shown in **Figure 6d**. Stable performance was observed over 10000 s without a decline in current density. The overall OER performance of synthesized

$\text{CoFe}_2\text{O}_4/\text{Co}_3\text{O}_4$ nanostructure catalyst and reported RuO_2 is compared in **Table 1**. The high OER performance of $\text{CoFe}_2\text{O}_4/\text{Co}_3\text{O}_4$ nanostructure is attributed to the synergistic effect

of CoFe_2O_4 and Co_3O_4 , which accelerated the charge transfer between active sites and intermediates.

4. CONCLUSIONS

In conclusion, we have demonstrated the application of $\text{CoFe}_2\text{O}_4/\text{Co}_3\text{O}_4$ nanostructure for OER performance. Owing to the enhanced conductivity and quick reaction dynamics, the $\text{CoFe}_2\text{O}_4/\text{Co}_3\text{O}_4$ nanostructure electrocatalyst yielded high catalytic activity. The catalyst exhibited a low overpotential of 311 mV @10 mA/cm², a small Tafel slope of 87 mV/dec, and excellent long-term durability. The OER activities of transition metal oxides are dependent on the oxidation state, the number of 3d electrons of the metal atom as well as the binding energies of the oxygen atoms. Especially, the multivalent oxidation states $\text{M}^{+2/+3/+4}$ of $\text{CoFe}_2\text{O}_4/\text{Co}_3\text{O}_4$ were responsible for the creation of additional active sites in the hybrid system proving it to be an excellent candidate for oxygen evolution reactions. The increased number of active sites and synergistic effect enhanced the OER performance of the $\text{CoFe}_2\text{O}_4/\text{Co}_3\text{O}_4$ nanostructure. With the merit of cost-effective, earth-abundant, and efficient OER performance, $\text{CoFe}_2\text{O}_4/\text{Co}_3\text{O}_4$ nanostructure could be a promising non-noble electrocatalyst for water splitting.

ACKNOWLEDGMENTS

The authors would like to acknowledge financial support from SERB Early Career Research project (Grant No. ECR/2017/001850), Department of Science and Technology (DST/NM/NT/2019/205(G); DST/TDT/SHRI-34/2018), Karnataka Science and Technology Promotion Society (KSTePS/VGST-RGS-F/2018-19/GRD NO. 829/315), start-up grant, Jain University (11 (39)/17/013/2017SG), Nanomission (SR/NM/NS-20/2014) for the characterization facilities.

REFERENCES

[1] M. I. Jamesh, Y. Kuang, X. Sun, Constructing Earth-abundant 3D Nanoarrays for Efficient Overall Water Splitting—A Review, *ChemCatChem* **11**, 1550-1575, (2019).

- [2] J. Song, C. Wei, Z.F. Huang, C. Liu, L. Zeng, X. Wang, Z.J. Xu, A review on fundamentals for designing oxygen evolution electrocatalysts, *Chemical Society Reviews* **49**, 2196-2214, (2020).
- [3] P. Shinde, C.S. Rout, D. Late, P.K. Tyagi, M.K. Singh, Optimized performance of nickel in crystal-layered arrangement of $\text{NiFe}_2\text{O}_4/\text{rGO}$ hybrid for high-performance oxygen evolution reaction, *International Journal of Hydrogen Energy*, **46**, 2617-2629, (2021).
- [4] Y. Ma, H. Zhang, J. Xia, Z. Pan, X. Wang, G. Zhu, B. Zheng, G. Liu, L. Lang, Reduced $\text{CoFe}_2\text{O}_4/\text{graphene}$ composite with rich oxygen vacancies as a high efficient electrocatalyst for oxygen evolution reaction, *International Journal of Hydrogen Energy*, **45**, 11052-11061, (2020).
- [5] Q. Shi, C. Zhu, D. Du, Y. Lin, Robust noble metal-based electrocatalysts for oxygen evolution reaction, *Chemical Society Reviews*, **48**, 3181-3192, (2019).
- [6] L. Li, Y. Zhang, J. Li, W. Huo, B. Li, J. Bai, Y. Cheng, H. Tang, X. Li, Facile synthesis of yolk-shell structured ZnFe_2O_4 microspheres for enhanced electrocatalytic oxygen evolution reaction, *Inorganic Chemistry Frontiers*, **6**, 511-520, (2019).
- [7] Y. Liu, Z. Niu, Y. Lu, L. Zhang, K. Yan, Facile synthesis of CuFe_2O_4 crystals efficient for water oxidation and H_2O_2 reduction, *Journal of Alloys and Compounds*, **735**, 654-659, (2018).
- [8] H.Y. Wang, Y.Y. Hsu, R. Chen, T.S. Chan, H.M. Chen, B. Liu, Ni^{3+} -induced formation of active NiOOH on the spinel Ni-Co oxide surface for efficient oxygen evolution reaction, *Advanced Energy Materials*, **5**, 1500091, (2015).
- [9] M. Sun, D. Lin, S. Wang, T. Zhang, D. Wang, J. Li, Facile synthesis of $\text{CoFe}_2\text{O}_4\text{-CoFe}_x/\text{C}$ nanofibers electrocatalyst for the oxygen evolution reaction, *Journal of The Electrochemical Society*, **166**, H412, (2019).
- [10] X. Chen, X. Zhang, L. Zhuang, W. Zhang, N. Zhang, H. Liu, T. Zhan, X. Zhang, X. She, D. Yang, Multiple Vacancies on (111) Facets of Single-Crystal NiFe_2O_4 Spinel Boost Electrocatalytic Oxygen Evolution Reaction, *Chemistry—An Asian Journal*, **15**, 3995-3999, (2020).
- [11] Z. Zhang, D. Zhou, S. Zou, X. Bao, X. He, One-pot synthesis of $\text{MnFe}_2\text{O}_4/\text{C}$ by microwave sintering as an efficient bifunctional electrocatalyst for oxygen reduction and oxygen evolution reactions, *Journal of Alloys and Compounds*, **786**, 565-569, (2019).
- [12] J.A. Rajesh, B.K. Min, J.H. Kim, H. Kim, K.S. Ahn, Cubic spinel AB_2O_4 type porous ZnCo_2O_4 microspheres: facile hydrothermal synthesis and their electrochemical performances in pseudocapacitor, *Journal of The Electrochemical Society*, **163**, A2418, (2016).
- [13] V.D. Silva, L.S. Ferreira, T.A. Simões, E.S. Medeiros, D.A. Macedo, 1D hollow MFe_2O_4 (M= Cu, Co, Ni) fibers by Solution Blow Spinning for oxygen evolution reaction, *Journal of colloid and Interface Science*, **540**, 59-65, (2019).
- [14] Y. Chen, Z. Shi, S. Li, J. Feng, B. Pang, L. Yu, W. Zhang, L. Dong, N, S-codoped graphene supports for Ag-Mn Fe_2O_4 nanoparticles with improved

- performance for oxygen reduction and oxygen evolution reactions, [*Journal of Electroanalytical Chemistry*, **860**, 113930, \(2020\).](#)
- [15] T. Li, Y. Lv, J. Su, Y. Wang, Q. Yang, Y. Zhang, J. Zhou, L. Xu, D. Sun, Y. Tang, Anchoring CoFe₂O₄ nanoparticles on N-doped carbon nanofibers for high-performance oxygen evolution reaction, [*Advanced Science*, **4**, 1700226, \(2017\).](#)
- [16] D. Xu, B. Liu, G. Liu, K. Su, C. Yang, H. Tong, D. Qian, J. Li, N-doped bamboo-like CNTs combined with CoFe–CoFe₂O₄ as a highly efficient electrocatalyst towards oxygen evolution, [*International Journal of Hydrogen Energy*, **45**, 6629-6635, \(2020\).](#)
- [17] Z. Rahimi, H. Sarafraz, G. Alahyarizadeh, A.S. Shirani, Hydrothermal synthesis of magnetic CoFe₂O₄ nanoparticles and CoFe₂O₄/MWCNTs nanocomposites for U and Pb removal from aqueous solutions, [*Journal of Radioanalytical and Nuclear Chemistry*, **317**, 431-442, \(2018\).](#)
- [18] V.P. Senthil, J. Gajendiran, S.G. Raj, T. Shanmugavel, G.R. Kumar, C.P. Reddy, Study of structural and magnetic properties of cobalt ferrite (CoFe₂O₄) nanostructures, [*Chemical Physics Letters*, **695**, 19-23, \(2018\).](#)